PROCEEDINGS, Fourteenth Workshop on Geothermal Reservoir Engineering
Stanford University, Stanford, California, January 24-26, 1989
SGP-TR-122

LBL-26509

ON RELATIVE PERMEABILITY OF ROUGH-WALLED FRACTURES

K. Pruess and Y. W. Tsang

Earth Sciences Division
Lawrence Berkeley Laboratory
1 Cyclotron Road
Berkeley, California 94720

and

Department of Materials Science and Mineral Engineering
University of California, Berkeley

ABSTRACT

This paper presents a conceptual and numerical model of multiphase flow in fractures. The void space of real rough-walled rock fractures is conceptualized as a two-dimensional heterogeneous porous medium, characterized by aperture as a function of position in the fracture plane. Portions of a fracture are occupied by wetting and non-wetting phase, respectively, according to local capillary pressure and accessibility criteria. Phase occupancy and permeability are derived by assuming a parallel-plate approximation for suitably small subregions in the fracture plane. Wetting and non-wetting phase relative permeabilities are calculated by numerically simulating single phase flows separately in the wetted and non-wetted pore spaces. Illustrative examples indicate that relative permeabilities depend sensitively on the nature and range of spatial correlation between apertures.

INTRODUCTION

Most high-temperature geothermal reservoirs are situated in formations with predominant fracture permeability. In many of these systems two-phase flow of liquid water and vapor occurs in the fractures naturally, or will be induced from boiling in response to fluid production. Geothermal wells will usually produce at commercially viable rates only if they intercept sufficiently permeable fracture zones. Multiphase flow in fractures also occurs in oil and gas production, and in the vicinity of geologic repositories for heat-generating nuclear wastes.

When analyzing multiphase flows it is important to carefully distinguish between fluid phases and components. Liquid water and water vapor constitute a single-component two-phase system, while mixtures of water and oil, or water and natural gas, are two phase systems consisting of at least two components. (Oil and natural gas themselves may contain many different components or chemical species). Single-component two-phase systems may behave rather differently than their two-component counterparts. For example, a gas (vapor) phase can evolve inside a body of liquid water by phase transformation (boiling) in response to suitable changes in temperature or pressure. The vapor phase need not be geometrically connected to a contiguous body of vapor. This is in contrast to two-component two-phase systems, where the phase composition in a region can only change if an invading phase can access the region through a continuous flow path. In addition to issues of phase occupancy, phase mobilities are also different in single-component two-phase systems. Through a thermodynamic analysis, Verma (1986) showed that vapor bubbles cannot get trapped at pore throats in concurrent vapor-liquid flow, while under suitable capillary pressure conditions the non-wetting phase in a two-component system may get trapped.

Given the wide occurrence and practical importance of multiphase flows in fractures, it is surprising that very little quantitative information on such flows is available. Experimental work has demonstrated multiphase flow effects in fractures (Barton, 1972; Bawden and Roegiers, 1985), but we are not aware of any measurements of fracture relative permeabilities in the literature. The lack of laboratory data is probably due to difficulties in controlling and measuring phase saturations in fractures. Standard laboratory techniques such as gamma ray or microwave attenuation devices are sensitive to the volumetric composition of a multiphase system. The void volumes present in fractures, however, are invariably small compared to sample volumes and interstitial voids in unfractured material, so that the application of volumetric methods meets with great difficulties and inaccuracies.

From a theoretical viewpoint the subject of multiphase flow in fractures has also received very little attention. The chief obstacle here seems to be that until recently there was a lack of credible models for pore space geometry in natural rock fractures. Evans and coworkers have used capillary theory to study the multiphase flow behavior of systems of idealized parallel-plate fractures (Evans, 1983; Evans and Huang, 1983; Rasmussen et al., 1985), and of wedge-shaped fractures with continuously varying apertures (Rasmussen, 1987). Newly developed

imaging techniques (Gentier, 1986; Pyrak-Nolte et al., 1987; Hakami, 1988) have led to the conceptualization of fractures as two-dimensional heterogeneous porous media, with flow taking place in intersecting channels of varying aperture (Tsang and Tsang, 1987; Wang et al., 1988; Montazer et al., 1988). These emerging concepts open the way for new theoretical approaches to multiphase flow in fractures.

TWO-DIMENSIONAL POROUS MEDIA

In the hydrologic literature fractures have often been idealized as the void space enclosed between two parallel plates. "Real" rock fractures, however, have rough surfaces with numerous contact points. Recent observations indicate that the topography of fracture walls may have fractal structure (Brown and Scholz, 1985; Wang et al., 1988). In this paper we focus on "small" fractures in hard rock, with apertures typically in the submillimeter range, as opposed to fracture zones which consist of a layer of highly permeable material sandwiched between rock of low permeability. Fracture zones may have widths of order 0.1 to 1 m and have a three-dimensional pore structure. In contrast, the small fractures considered here consist of the void space enclosed between two impermeable surfaces, which in a topological sense constitutes a two-dimensional porous medium. Quantitatively this can be described by specifying the two boundary surfaces, $z_i = z_i(x,y)$ for $i = 1, 2$. Alternatively, one can specify the midplane $z = (z_1 + z_2)/2$ and the local aperture $b(x,y) = z_2 - z_1$. For simplicity we assume fractures to be planar in the following (z = const.); however, this assumption is made only for convenience and is not necessary for our model. The important property of the fracture model developed here is the two-dimensional nature of the pore space.

Several different techniques have been used to experimentally characterize apertures of rough-walled fractures, including linear profilometer scans (e.g. Gentier, 1986), two-dimensional imaging from replicas of the pore space made by injection of Woods' metal or epoxy resins (Pyrak-Nolte et al., 1987; Gale, 1987; Gentier et al., 1989), and application of fluid drops of known volume (Hakami, 1988). Different scales of spatial correlation among apertures have been noted experimentally (Gentier, 1986). In various instances fracture apertures have been found to follow a skewed distribution well approximated by a log-normal distribution (Gentier, 1986; Gale, 1987; Hakami, 1988). Figures 1 and 2 show examples of fracture pore spaces simulated by computer (see below).

Adopting a finite spatial resolution $\Delta x \times \Delta y$ results in a discretized representation of fracture apertures, with average aperture being b_{ij} in the element $(x_i - \Delta x/2, x_i + \Delta x/2; y_j - \Delta y/2, y_j + \Delta y/2)$ of the fracture plane. In the calculations reported below we use a 20×20 grid to discretize a 40mm × 40mm portion of a fracture plane, so that $\Delta x = \Delta y = 2$mm (Figures 3 and 4). For convenience, we will use a shorthand notation (i,j) for an element of the fracture plane. Discretized representations of fracture apertures can be generated from continuous distributions through stochastic techniques, or they can be directly obtained from laboratory specimen by digitizing pore space images into a finite number of "pixels".

In the present study, we use geostatistical methods to generate discretized aperture distributions in the fracture plane. In most cases we use a lognormal distribution of apertures with an exponential spatial covariance. The aperture generation code COVAR (William and El-Kadi, 1986) was modified to allow for anisotropic covariance. The input parameters to the aperture generation code are $\log b_0$, σ, λ_x, and λ_y, which denote, respectively, the mean and standard deviation of the lognormal distribution, and the spatial correlation lengths in x and y directions.

Figures 1 and 2 show stochastic realizations of lognormal aperture distributions in a fracture plane with different length and anisotropy of spatial correlation. The parameters for these distributions are given in Table 1, and the discretized counterparts are shown in Figures 3 and 4.

RELATIVE PERMEABILITY MODEL

It is well established that for single-phase flow the permeability of a parallel-plate fracture of aperture b is given by

$$k = \frac{b^2}{12} \tag{1}$$

This permeability is present over a flow sheet of width b so that, when normalized to a unit thickness perpendicular to the fracture, the average permeability is

$$\bar{k} = \frac{b^3}{12} \tag{2}$$

whence the term "cubic law" for this relationship. In two-phase conditions, the capillary pressure between wetting and non-wetting phases is given by

$$P_c = \frac{2\gamma \cdot \cos\alpha}{b} \tag{3}$$

where γ is the surface tension between wetting and non-wetting phases, and α is the contact angle between the wetting phase meniscus and the fracture wall. We adopt the convention of taking $P_c > 0$, and we assume that the contact angle for water-vapor (or wetting-nonwetting phase) is 0.

The crucial concept developed in this paper can now be stated as follows: As far as multiphase flow properties are concerned, a rough-walled fracture with position-

dependent aperture is assumed to behave locally like a parallel-plate fracture with the same average aperture (Brown, 1987). Thus, a fracture element with aperture b_{ij} has a single-phase permeability $b_{ij}^2/12$, and its phase occupancy is governed by the local capillary pressure $P_{ij} = 2\gamma/b_{ij}$. In "quasistatic" conditions of low pressure gradients (low capillary number), when both wetting and non-wetting phase have access to the fracture element (i,j), it will contain wetting phase if $P_c < P_{ij}$, non-wetting phase if $P_c > P_{ij}$. Note that this assumption ignores possible effects from wetting phase which may be held by small-scale roughness or by adsorptive forces in the walls of fracture elements the bulk of which would be drained (Pruess et al., 1988). Mineral coatings may also play a role in complicating phase occupancy and mobility (N.G.W. Cook, private communication).

Our procedure for calculating capillary pressures and relative permeabilities can now be described as follows.

(1) Obtain a discretized representation b_{ij} of fracture apertures for a finite rectangular domain, either by generating a stochastic realization of a suitable aperture distribution, or by directly digitizing an image of the pore space (see Figures 3 and 4).

(2) Define a cutoff-aperture b_c, corresponding to a capillary pressure $P_c = 2\gamma/b_c$, and occupy all apertures smaller than b_c with wetting phase, all larger apertures with non-wetting phase. (This occupancy rule ignores global accessibility criteria which may be very important in two-component flow; it is appropriate for single-component vapor-liquid systems.) Calculate the saturation S_{cw} (and $S_{cnw} = 1 - S_{cw}$) corresponding to the cutoff capillary pressure P_c by directly summing the wetted pore volume.

(3) Apply suitable constant-pressure conditions at the boundaries of the fracture, and simulate fluid flow in the network of occupied fracture elements. (In our simulations, flow is taking place in the x-direction, with no-flow boundaries at y = 0 and y = 1; see Figures 3 and 4.) The steady-state flow rate obtained when only apertures less than b_c are occupied will yield the effective wetting phase permeability; a similar simulation with only apertures larger than b_c occupied will yield the effective non-wetting phase permeability. It should be noted that it is only under conditions of small capillary number that the two-phase flow problem in the fracture plane separates into two single-phase flow problems. When sizeable pressure gradients are present the flowing phases will be able to invade otherwise "forbidden" pores.

(4) Division of the effective phase permeability by the single-phase permeability (all apertures occupied) yields the relative permeability at saturation S_{cw}. Repeat the procedure for a range of b_c (and S_{cw}) to obtain the entire relative permeability and capillary pressure curves.

NUMERICAL SIMULATIONS

In order to implement the procedure outlined above it is necessary to derive the transmissivity between fracture elements of different aperture. Consider a "connection" (flow contact) between two fracture elements with apertures b_n and b_m, respectively (Figure 5). Neglecting non-linear flow effects at the juncture, the total pressure drop between n and m can be expressed as

$$\begin{aligned} P_n - P_m &= (P_n - P_i) + (P_i - P_m) \\ &= F_{mn} \frac{\mu}{\rho} \left\{ \frac{D_n}{k_n A_n} + \frac{D_m}{k_m A_m} \right\} \end{aligned} \tag{4}$$

Here P_i denotes the pressure at the interface, F_{mn} is the mass flow rate, μ is fluid viscosity, ρ is density, and D_n, k_n, A_n are nodal distance, permeability, and cross-sectional area for flow in fracture element n, respectively (likewise for element m). Introducing an effective permeability k_{mn} and connection area A_{mn}, the pressure drop can also be written as

$$P_n - P_m = F_{mn} \frac{\mu}{\rho} \frac{D_n + D_m}{k_{mn} A_{mn}} \tag{5}$$

Equating the expressions (4) and (5), and inserting for flow area $A_n = b_n \times \Delta y$, similarly for A_m, and using Eq. (1) for permeability, we obtain

$$k_{mn} A_{mn} = \frac{(D_n + D_m)\Delta y}{12 \left\{ \frac{D_n}{b_n^3} + \frac{D_m}{b_m^3} \right\}} \tag{6}$$

indicating that only the product of effective interface permeability k_{mn} and interface area A_{mn} is defined. For the numerical implementation we find it convenient to take $k_{mn} = k = \text{const.}$ for all flow connections. With this convention we obtain

$$A_{mn} = \frac{(D_n + D_m)\Delta y}{12k \left\{ \frac{D_n}{b_n^3} + \frac{D_m}{b_m^3} \right\}} \tag{7}$$

for "active" (occupied) connections; $A_{mn} = 0$ for inactive connections.

We have incorporated these equations into our general-purpose simulator "MULKOM" (Pruess, 1983, 1988). Additional minor code changes were made to improve the calculational efficiency for small fracture domains, in which individual fracture elements, represented as separate grid blocks, have small linear dimensions of order 1 mm. The modifications include specification of a fictitious very large fluid viscosity (of order 10^6 Pa·s) to scale up pressure differences between neighboring grid blocks and thereby diminish numerical cancellation errors, and automatic adjustment of time step and convergence criteria to expedite and recognize attainment of a steady state. From the numerical simulation we obtain

the total steady-state flow rate F across the fracture between boundaries separated by a distance L and held at a pressure difference of ΔP. A straightforward application of Darcy's law gives the following expression for effective permeability

$$k = \frac{F}{A} \frac{\mu}{\rho} \frac{L}{\Delta P} \qquad (8)$$

The permeability in Eq. (8) is normalized to a cross-sectional area A, which we take to be $1\,m^2$; i.e., it is assumed that the modeled fracture segment is embedded in a cross-sectional area of $1 \times 1\,m^2$.

RESULTS AND DISCUSSION

The accuracy of the numerical simulation procedure was verified by comparison with computations using an electric resistor analog. Simulations were then performed for a number of discretized realizations of lognormal and normal aperture distributions with different mean values and spatial correlation lengths. Figures 6 and 7 show results for wetting and nonwetting phase relative permeabilities, respectively, for the two aperture distributions of Figures 3 and 4 (parameters as given in Table 1). The different data points in Figures 6 and 7 correspond to different cutoff apertures b_c.

Before discussing the simulation results presented in Figures 6 and 7 it should be emphasized that these are to be considered a first rough illustration of the trends; due to various approximations and idealizations involved they are not expected to provide a quantitatively valid evaluation of fracture relative permeabilities. The test calculations performed so far indicate that relative permeability predictions depend sensitively on the details of spatial correlation between apertures; a realistic description of these correlations is required before quantitatively useful results can be obtained. Other limitations arise from the stochastic nature of the aperture distributions; calculations for a reasonably large number of realizations would be needed before firm conclusions can be drawn. The rather coarse discretization (20×20) of the fracture plane and the five-point finite difference scheme used here result in grid orientation errors (Forsythe and Wasow, 1960; Yanosik and McCracken, 1979). By restricting flow connections to the four nearest neighbors with a shared interface, the five-point scheme will produce an overestimate of flow interference between phases.

The most remarkable feature of the relative permeability curves shown in Figure 6 is the apparent strong interference between the phases: Immobile nonwetting phase saturation is extremely large, about 84%, and a saturation "window" in which both phases would be mobile is virtually non-existent. This contrasts with the behavior shown in Figure 7, where immobile nonwetting saturation is a more modest (although still large) 51.5%, and there is a considerable range of saturations over which both phases can flow simultaneously. In our calculations so far we have generally found that a significant window of two-phase mobility exists only for anisotropic aperture distributions, with considerably larger spatial correlation length in the direction of flow than perpendicular to it.

Our wetting phase relative permeabilities appear to be generally similar to experimental results for (three-dimensional) porous media (Osoba et al., 1951; Johnson et al., 1959; Brooks and Corey, 1964), while non-wetting phase relative permeabilities are predicted to drop off rather rapidly with increasing wetting phase saturation.

This can be understood from the characteristics of the lognormal distribution, in which there are many relatively small apertures and a small number of large apertures. In the absence of long-range spatial correlations between apertures (see Figure 1), a contiguous flow path for nonwetting phase can only be maintained when in addition to all the large apertures also some of the smaller apertures contain nonwetting phase. In other words, a relatively large nonwetting phase saturation is required before nonwetting phase can flow.

Phase interference is generally stronger in two-dimensional than in three-dimensional porous media, because there are fewer alternative routes for bypassing inaccessible pores. (In percolation theory parlance, two-dimensional media have a smaller coordination number). Anisotropic spatial correlation, with larger correlation length in the direction of flow, tends to segregate the small aperture and the large aperture pathways (see Figure 2). This diminishes phase interference and broadens the saturation window for two-phase mobility (Figure 7). The sudden jump in non-wetting phase relative permeability at $S_W = 48.5\%$ occurs because of a single pore throat located near $x = 0.5$, $y = 0.3$ (see Figures 2 and 4).

At the present time there are no reliable observational data with which our predictions for fracture relative permeabilities can be compared. However, there is some evidence from fractured geothermal reservoirs which suggests that the sum of liquid and vapor relative permeabilities is close to 1 over the entire range of saturations (Grant, 1977; Pruess et al., 1983, 1984; Bodvarsson et al., 1987). Such behavior is not necessarily in disagreement with our findings; in fact, it is straightforward to identify geometric characteristics of fracture aperture distributions that would lessen or completely eliminate interference between phases, and thereby give rise to larger wetting and nonwetting phase relative permeabilities at intermediate saturations.

For example, it is quite conceivable that fractures commonly have certain long-range spatial correlations between apertures. These could be provided by channels or rivulets formed by mechanical erosion or mineral dissolution processes. Another possibility is that field-determined relative permeabilities could pertain to an aggregate response of several fractures of different magnitude, with wetting phase flowing in the smaller frac-

tures, nonwetting phase in the larger ones. Under such conditions of segregated flow the sum of wetting and nonwetting phase relative permeabilities would be near 1 at all levels of saturation.

In addition to geometric characteristics of the fracture pore space, there is a purely thermodynamic effect that could enhance nonwetting phase permeability in single-component two-phase flow. As was shown by Verma (1986), phase transformation effects will prevent vapor bubbles from getting trapped at pore throats in concurrent vapor-liquid flow. Verma's analysis indicates that phase change processes will in effect enable vapor flow to take place even if there is no contiguous flow path for the vapor phase. This effect would generally enhance nonwetting phase relative permeability in single-component two-phase systems (a volatile fluid and its vapor) in comparison to two-component systems.

CONCLUDING REMARKS

We have developed a new conceptual approach for wetting and nonwetting phase relative permeabilities in real rough-walled rock fractures. Our method utilizes a quantitative description of the fracture pore space in terms of an aperture distribution, which can be obtained either through direct laboratory measurements on fracture specimens, or by means of stochastic computer-generated realizations of mathematical distribution functions. The crucial concept used in our method is that the capillary and permeability properties of a fracture can be approximated by a parallel-plate model locally. This is a hypothesis which requires further experimental and theoretical study.

First applications of the method involved computer simulation of flow in fractures with synthetic (lognormal) aperture distributions. It was found that interference between phases is generally strong. The sum of wetting and nonwetting phase relative permeabilities is much less than 1 at intermediate saturations, unless there are long-range spatial correlations among apertures in the direction of flow. Such correlations are likely to occur commonly in fractures in the form of channels or rivulets. Even so, first results seem to indicate that immobile nonwetting phase saturations in fractures may be large, of order 50%. However, this result may only be applicable to two-component two-phase systems, such as water and gas (or air), or water and oil. In geothermal reservoirs we are dealing with essentially single-component (water) two-phase systems. In these systems phase change provides an additional degree of freedom in two-phase flow, which will diminish or eliminate blocking of one phase by the other, and thereby enhance nonwetting phase relative permeability. Contributions from matrix flow, neglected in this paper, will also tend to lessen phase interference.

There is some evidence from fractured geothermal reservoirs that the sum of liquid and vapor relative permeabilities is close to 1 at all saturations. We suggest that this feature may be due to the indicated phase transformation effects rather than due to fracture flow, as has often been assumed in the geothermal literature. All else being equal, the sum of wetting and nonwetting phase relative permeabilities at intermediate saturations should be smaller in fractures than in three-dimensional porous media, because of the reduced possibility for bypassing inaccessible pores.

The relative permeability functions shown in Figures 6 and 7 were obtained for highly idealized aperture distributions, with no explicit allowance for phase change effects in vapor-liquid flow. They are not expected to give a realistic outlook on relative permeabilities in fractured geothermal reservoirs. Work is continuing to apply the method developed in this paper to conditions and parameters of practical interest.

ACKNOWLEDGEMENT

For a careful review of the manuscript and the suggestion of improvements, the authors are indebted to M. Lippmann and J. Wang. This work was supported by the Geothermal Technology Division, U.S. Department of Energy, under Contract No. DE-AC03-76SF00098.

REFERENCES

Barton, N. R. (1972). "A Model Study of Air Transport from Underground Openings Situated Below Groundwater Level," Proceedings, Symposium International Society for Rock Mechanics, Stuttgart, pp. T3-A1-T3-A20.

Bawden, W. F. and J. C. Roegiers (1985). "Gas Escape from Underground Mined Storage Facilities - A Multiphase Flow Phenomenon", Proceedings, International Symposium on Fundamentals of Rock Joints, Björkliden, 15-20 September, pp. 503-514.

Bodvarsson, G. S., K. Pruess, V. Stefansson, S. Björnsson, and S. B. Ojiambo (1987). "East Olkaria Geothermal Field, Kenya. 1. History Match with Production and Pressure Decline Data", *Journal of Geophys. Res., 92,* (B1) 521-539.

Brooks, R. H. and A. T. Corey (1964). "Hydraulic Properties of Porous Media", Hydrol. Paper 3, Civ. Eng. Dept., Colorado State University, Fort Collins, CO., 27 pp.

Brown, S. R. (1987). "Fluid Flow Through Rock Joints: The Effect of Surface Roughness", *Journal of Geophys. Res., 92,* (B2) 1337-1347.

Brown, S. R. and C. H. Scholz (1985). "Broad Bandwidth Study of the Topography of Natural Rock Surfaces", *Journal of Geophys. Res., 90,* 12,575-12,582.

Evans, D. D. (1983). "Unsaturated Flow and Transport through Fractured Rock - Related to High-Level Waste Repositories", Final Report - Phase I, Department of Hydrology and Water Resources, University of Arizona, prepared for U. S. Nuclear Regulatory Commission, Report NUREG/CR-3206, March.

Evans, D. D. and C. H. Huang (1983). "Role of Desaturation on Transport through Fractured Rock", in *Role of the Unsaturated Zone in Radioactive and Hazardous Waste Disposal*, J. W. Mercer, P. S. C. Rao, and I. W. Marine (editors), Ann Arbor Science, pp. 165-178.

Forsythe, G. E. and W. R. Wasow (1960). *Finite-Difference Methods for Partial Differential Equations*, John Wiley and Sons, Inc., New York, London.

Gale, J. E. (1987). "Comparison of Coupled Fracture Deformation and Fluid Flow Models with Direct Measurements of Fracture Pore Structure and Stress-Flow Properties", Proceedings, 28th U. S. Symposium on Rock Mechanics, Tucson, AZ, June 29-July 1, pp. 1213-1222.

Gentier, S. (1986). Morphologie et Comportement Hydromécanique d'une Fracture Naturelle dans un Granite Sous Contrainte Normale, Doctoral Thesis, Université d'Orléans, Orléans, France.

Gentier, S., D. Billaux and L. van Vliet (1989). "Laboratory Testing of the Voids of a Fracture", to appear in *Int. Jour. Rock Mech. and Rock. Eng.*

Grant, M. A. (1977). "Permeability Reduction Factors at Wairakei", paper 77-HT-52, presented at AICHE-ASME Heat Transfer Conference, Salt Lake City, Utah, August.

Hakami, E. (1988). Water Flow in Single Rock Joints, Licentiate Thesis, Lulea University of Technology, Lulea, Sweden, November.

Johnson, E. F., D. P. Bossler and V. O. Narmann (1959). "Calculation of Relative Permeability from Displacement Experiments", *Trans., AIME, 216*, 370-376.

Montazer, P., F. Thamir and P. Harrold (1988). "Anisotropic Relative Permeability in a Plane Fracture", paper presented at International Conference on Fluid Flow in Fractured Rocks, Atlanta, GA, May 15-18.

Osoba, J. S., J. G. Richardson, J. K. Kerner, J. A. Hafford and P. M. Blair (1951). "Laboratory Measurements of Relative Permeability", *Pet. Trans., AIME*, 47-55.

Pruess, K. (1988). "SHAFT, MULKOM, TOUGH: A Set of Numerical Simulators for Multiphase Fluid and Heat Flow", *Geotermia, Rev. Mex. Geoenergia, 4*, (1) 185-202 (also: Lawrence Berkeley Laboratory Report LBL-24430).

Pruess, K. (1983). "Development of the General Purpose Simulator MULKOM", Annual Report 1982, Earth Sciences Division, Lawrence Berkeley Laboratory Report LBL-15500.

Pruess, K., G. S. Bodvarsson and V. Stefansson (1983). "Analysis of Production Data from the Krafla Geothermal Field, Iceland", paper presented at Ninth Workshop on Geothermal Reservoir Engineering, Stanford University, Stanford, CA, December.

Pruess, K., G. S. Bodvarsson, V. Stefansson and E. T. Eliasson (1984). "The Krafla Geothermal Field, Iceland, 4. History Match and Prediction of Individual Well Performance", *Water Resources Research, 20*, (11) 1561-1584.

Pruess, K., J. S. Y. Wang and Y. W. Tsang (1988). On Thermohydrological Conditions near High-Level Nuclear Wastes Emplaced in Partially Saturated Fractured Tuff. Part 2. Effective Continuum Approximation, Lawrence Berkeley Laboratory Report LBL-24564, January. (To appear in *Water Resources Research.)*

Pyrak-Nolte, L. J., L. R. Myer, N. G. W. Cook and P. A. Witherspoon (1987). "Hydraulic and Mechanical Properties of Natural Fractures in Low Permeability Rock", paper presented at Sixth International Congress on Rock Mechanics, Montreal, Canada, August.

Rasmussen, T. C. (1987). "Computer Simulation Model of Steady Fluid Flow and Solute Transport through Three-Dimensional Networks of Variably Saturated, Discrete Fractures", in D. D. Evans and T. J. Nicholson (eds.), Flow and Transport through Unsaturated Fractured Rock, Geophysical Monograph 42, American Geophysical Union, pp. 107-114.

Rasmussen, T. C., C. H. Huang and D. D. Evans (1985). "Numerical Experiments on Artificially-Generated, Three-Dimensational Fracture Networks: An Examination of Scale and Aggregation Effects", in International Association of Hydrogeologists (ed.), Memoirs, Vol. XVII, pp. 676-682.

Tsang, Y. W. and C. F. Tsang (1987). "Channel Model of Flow through Fractured Media", *Water Resources Res., 23*, (3) 467-479, March.

Verma, A. K. (1986). Effects of Phase Transformation on Steam-Water Relative Permeabilities, Doctoral Dissertation, University of California, Berkeley, CA, March (also: Lawrence Berkeley Laboratory Report LBL-20594).

Wang, J. S. Y., T. N. Narasimhan and C. H. Scholz (1988). "Aperture Correlation of a Fractal Fracture", *Journal Geophys. Res., 93*, (B3) 2216-2224.

Williams, S. A. and A. I. El-Kadi (1986). COVAR - A Computer Program for Generating Two-Dimensional Fields of Autocorrelated Parameters by Matrix Decomposition, Report, International Groundwater Modeling Center, Holcomb Research Institute, Butler University, Indianapolis, Indiana.

Yanosik, J. L., and T. A. McCracken (1979). "A Nine-Point, Finite Difference Reservoir Simulator for Realistic Prediction of Adverse Mobility Ratio Displacements", *Soc. Pet. Eng. J.*, 253-262, August.

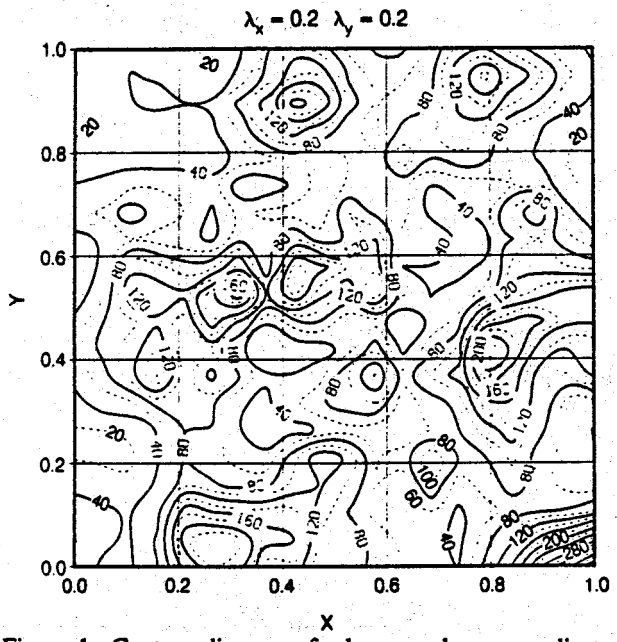

Figure 1. Contour diagram of a lognormal aperture distribution in a fracture plane with isotropic spatial correlation (Case 1, Table 1).

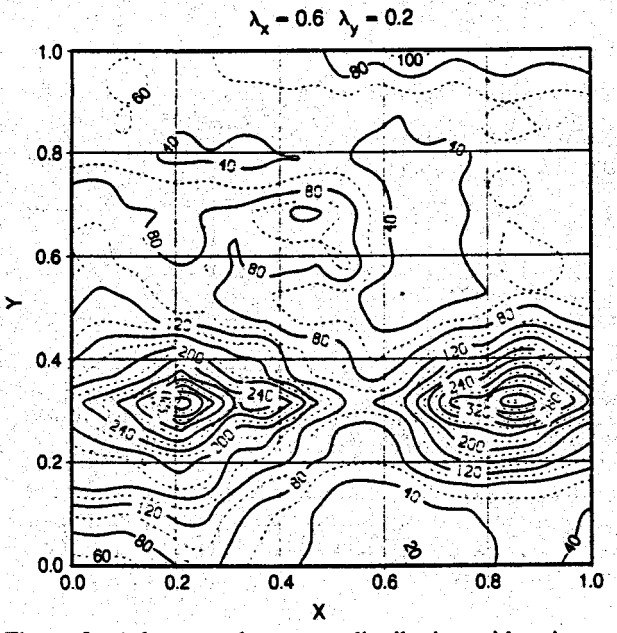

Figure 2. A lognormal aperture distribution with anisotropic spatial correlation (Case 2, Table 1).

Table 1. Parameters for lognormal aperture distributions

	Case 1	Case 2
mean aperture (μm)	81.8	81.8
standard deviation	0.43	0.43
x-spatial correlation	0.20	0.60
y-spatial correlation	0.20	0.20

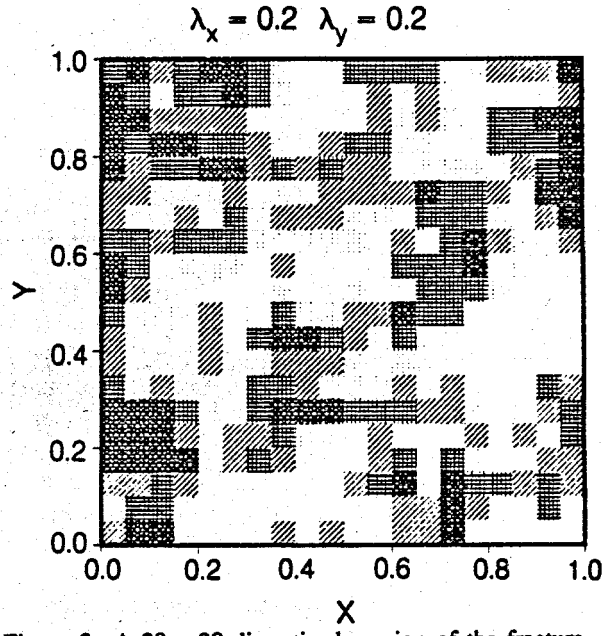

Figure 3. A 20 x 20 discretized version of the fracture apertures shown in Figure 1. Lighter shading corresponds to larger apertures.

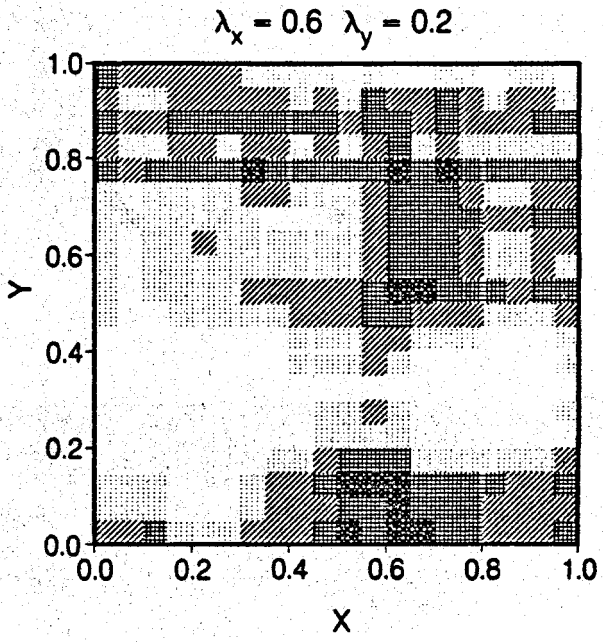

Figure 4. A 20 x 20 discretized version of the fracture apertures shown in Figure 2.

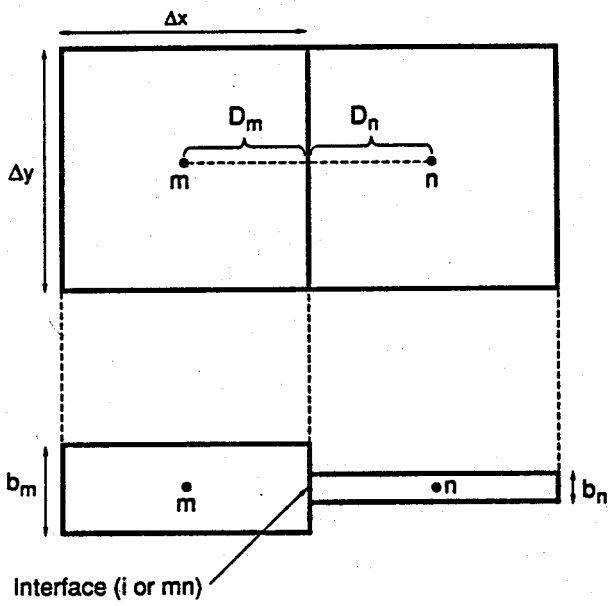

Figure 5. Schematic of a connection between two fracture elements, looking down onto the fracture plane (top), and giving an elevation view (bottom).

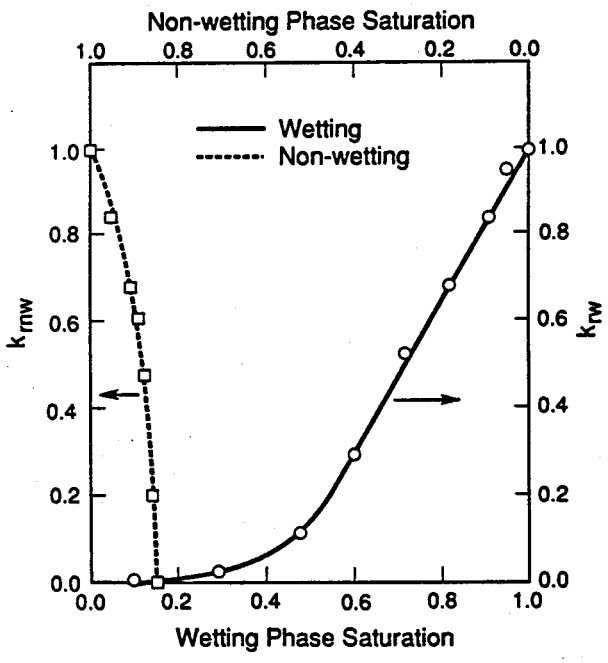

Figure 6. Simulated wetting and nonwetting phase relative permeabilities for the lognormal aperture distribution og Figures 1 and 3.

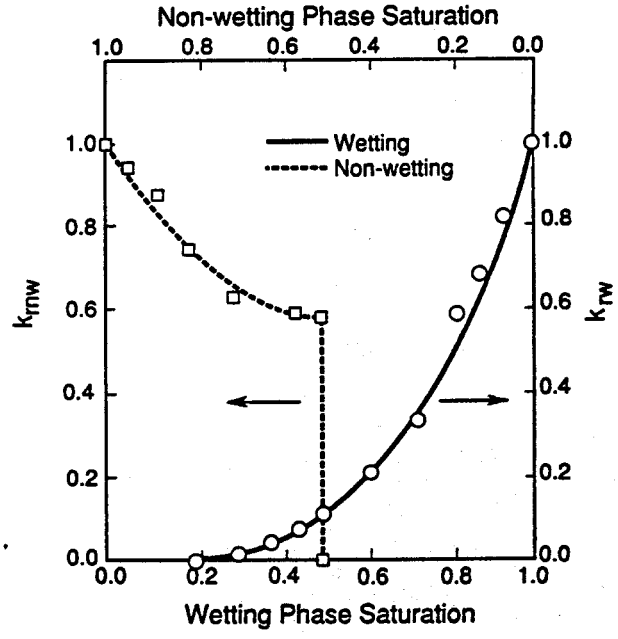

Figure 7. Simulated wetting and nonwetting phase relative permeabilities for the lognormal aperture distribution of Figures 2 and 4 with long-range anisotropic spatial correlation.